



ELSEVIER

Journal of Alloys and Compounds 330–332 (2002) 911–915

Journal of
ALLOYS
AND COMPOUNDS

www.elsevier.com/locate/jallcom

Operation of hydrogen–air fuel cells based on proton conducting oxides and hydrogen storage metals

S. Yamaguchi^{a,*}, H. Yugami^b, S. Ikeda^c^aResearch Institute, Chiba Institute of Technology, Narashino 275-0016, Japan^bFaculty of Engineering, Tohoku University, Sendai 980-8579, Japan^cHigh Energy Accelerator Research Organization, Tsukuba 305-0801, Japan

Abstract

We constructed a hydrogen–air fuel cell consisting of proton conducting oxides as an electrolyte and hydrogen storage metals as a hydrogen source. By using the hydrogen storage metals as the hydrogen source, we could test very easily both the electrolyte and the electrode materials. We tested three kinds of proton conducting oxides, i.e. $\text{SrCe}_{0.95}\text{Yb}_{0.05}\text{O}_{2.975}$, $\text{SrZr}_{0.9}\text{Yb}_{0.1}\text{O}_{2.95}$ and $\text{BaCe}_{0.9}\text{Y}_{0.1}\text{O}_{2.95}$ as well as two kinds of the negative electrode materials, i.e. graphite and nickel pastes. The fuel cell operated stably giving open circuit voltages of about 1.2 V, when the cell was maintained near a specific temperature at which hydrogen gas of about 0.1 MPa was released from the hydrogen storage metal. Under load, current densities varied depending on the kind of proton conducting oxides as well as on the negative electrode materials. Also the current densities varied with temperature and the thickness of electrolyte. The best current density–voltage performance was obtained from the fuel cells based on $\text{BaCe}_{0.9}\text{Y}_{0.1}\text{O}_{2.95}$ and nickel paste. The highest current density at 700 mV, 31.6 mA cm^{-2} , was delivered by a cell of 0.9 mm electrolyte thickness at 640°C. © 2002 Elsevier Science B.V. All rights reserved.

Keywords: Fuel cell; Proton conducting oxide electrolyte; Hydrogen storage metal

1. Introduction

The study and the development of hydrogen–air fuel cells are interesting and promising for power generation systems without the drain of fuel and the ecological problems. The use of a protonic conductor as a solid electrolyte for hydrogen–air fuel cells has distinctive features compared to that of an oxygen ion conductor like stabilized zirconias. When a protonic conductor is used instead of an oxygen ion conductor, fuel circulation is unnecessary in the case of the proton conductor, because no water molecules are generated at the hydrogen electrode. Furthermore, the operating temperature could be reduced to about 600°C so that fuel cells could be constructed from cheaper materials. Recently, acceptor-doped ABO_3 perovskite oxides ($\text{A}^{2+}=\text{Sr}, \text{Ba}, \text{Ca}$ and $\text{B}^{4+}=\text{Ce}, \text{Zr}$), which exhibit proton conduction, have received much attention as solid electrolytes of the hydrogen–air fuel cells. For examples, Takahashi and Iwahara [1] constructed fuel cells based on $\text{CaTiO}_3:\text{Mg}$, and

obtained current densities of $20\text{--}30 \text{ mA cm}^{-2}$ for a terminal voltage of 700 mV at 1000°C. Browell and Muller [2] obtained comparable results using $\text{SrZrO}_3:\text{Yb}$. Subsequently, Iwahara et al. [3,4] tested $\text{SrCeO}_3:\text{Yb}$ and obtained 20 and 50 mA cm^{-2} at temperatures 800 and 1000°C, respectively. More recently, Bonanos et al. [5] studied the fuel cell based on a disc of $\text{BaCeO}_3:\text{Gd}(10\%)$ and reported that the current densities for the electrode thickness of 1.2 mm were 6 and 30 mA at 700 mV at temperatures of 600 and 800°C, respectively, and the current densities varied inversely with electrode thickness.

In the previous work [6], we constructed an electrochemical cell consisting of proton conducting oxide as an electrolyte and hydrogen storage metal as a negative electrode, and examined hydrogen transport between the proton conducting oxide and the hydrogen storage metal. The EMF measurements of this cell demonstrated the feasibility of the new fuel cells based on the proton conducting oxide and the hydrogen storage metal. The present study aims to evaluate the performance of hydrogen–air fuel cells based on the proton conducting oxide and the hydrogen storage metal. Using hydrogen storage metal as the hydrogen source, a closed-type fuel cell which is not necessary to supply the hydrogen gas from outside

*Corresponding author. Tel.: +81-47-478-0588; fax: +81-47-478-0438.

E-mail address: yamasada@pf.it-chiba.ac.jp (S. Yamaguchi).

can be constructed. Our fuel cell operates safely without the danger of hydrogen explosion, and is allowed to exchange quickly both electrolyte and electrode materials. So we can examine very easily the performance of proton conducting oxides as the electrolyte of fuel cell. Three kinds of proton conducting oxides, e.g. $\text{SrCe}_{0.95}\text{Yb}_{0.05}\text{O}_{2.875}$, $\text{SrZr}_{0.9}\text{Yb}_{0.1}\text{O}_{2.95}$, and $\text{BaCe}_{0.9}\text{Y}_{0.1}\text{O}_{2.95}$ have been tested by obtaining their current density–voltage characteristics. Furthermore, graphite and nickel pastes are tested for their aptitude for the negative electrode (anode) material.

2. Experimental

The hydrogen–air fuel cell used in the present work is illustrated schematically in Fig. 1. Both electrode components were separated by the solid electrolyte. A disc-shaped polycrystalline oxide pellet of 15 mm diameter and 0.9–1.8 mm thickness was used as the electrolyte. The oxide pellet was prepared by a solid-state reaction and sintering process using appropriate oxides and carbonates as starting materials. Electrodes were formed by coating the faces of the pellets with conductive pastes. Silver paste backed with silver mesh was used for the positive electrode (cathode) and the contact lead of the positive electrode (cathode) was taken from the silver mesh. Graphite or nickel paste backed with nickel mesh was applied for the negative electrode (anode) and the contact lead of the negative electrode (anode) was connected to the nickel mesh. In this fuel cell, the hydrogen storage metal was used as the hydrogen source.

Although the positive component was exposed to air, the negative component which contained hydrogen storage metal was sealed tightly to prevent the release of hydrogen. The cell was situated in an electric furnace in order to release hydrogen from the hydrogen storage metal. For the cell operation at 600°C, TiH_2 hydride was used as hydrogen source. The voltage–current characteristics were measured by varying the external resistance, R_{ext} , in the electrical circuit shown in Fig. 2.

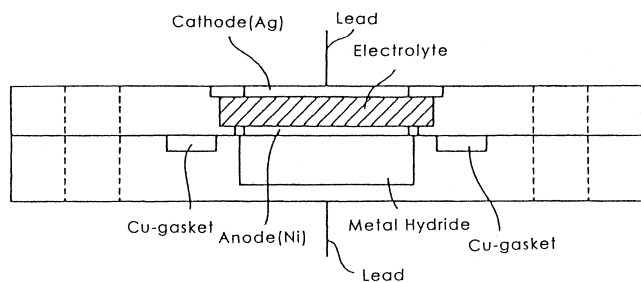


Fig. 1. Schematic illustration of hydrogen–air fuel cell consisting of proton conducting oxide as an electrolyte and hydrogen storage metal as hydrogen source.

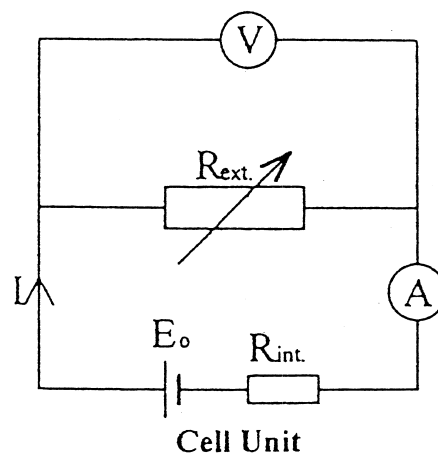


Fig. 2. Equivalent circuit for cell I – V measurement, where R_{ext} is the external resistance and R_{int} is the internal cell resistance. The output currents I are evaluated by the relation: $I = V/R_{\text{ext}}$, where the output voltages V are expressed by $V = E_0 - I \cdot R_{\text{int}}$.

3. Results and discussion

A distinct EMF is observed when hydrogen and oxygen gases are introduced to the negative electrode (anode) and positive electrode (cathode), respectively. If the electrolyte of this cell is a proton conductor, the proton has a tendency to migrate across the conductor to the positive electrode (cathode), where it discharges to form water vapor. The free energy change ΔG of this cell reaction, $\text{H}_2 + 1/2\text{O}_2 = \text{H}_2\text{O}$, determines the cell EMF, $E_0 = -\Delta G/2F$.

In the present study, a build-up of the EMF is observed when the hydrogen–air fuel cell is heated in the electric furnace. The EMF of the fuel cell responds to temperature, although it tends to saturate near a specific temperature at which the hydrogen gas of about 0.1 MPa is released from the hydrogen storage metal. The fuel cell consisting of the TiH_2 hydride as the hydrogen source operates stably near 600°C giving an open circuit voltage of about 1.2 V, which is consistent with the theoretical EMF (1.23 V) expected from the free energy change of this cell reaction. This result indicates that the transport number of protons: $t_p = \sigma_p/\sigma_t$ is close to unity, where σ_p and σ_t are protonic and total conductivity, respectively.

An example of the discharge characteristic under different loads for a fuel cell using $\text{BaCe}_{0.9}\text{Y}_{0.1}\text{O}_{2.95}$ as the electrolyte is shown in Fig. 3. Under load, the cell operated stably giving constant output currents and voltages. The output characteristics of this cell are measured by varying an external resistance, R_{ext} , from 10 to 100 k Ω to generate a set of correlated I – V reading. The following relations for the output current, I , and voltage, V , are deduced from the circuit,

$$V = E_0 R_{\text{ext}} / (R_{\text{ext}} + R_{\text{int}}), \quad (1)$$

$$I = E_0 / (R_{\text{ext}} + R_{\text{int}}), \quad (2)$$

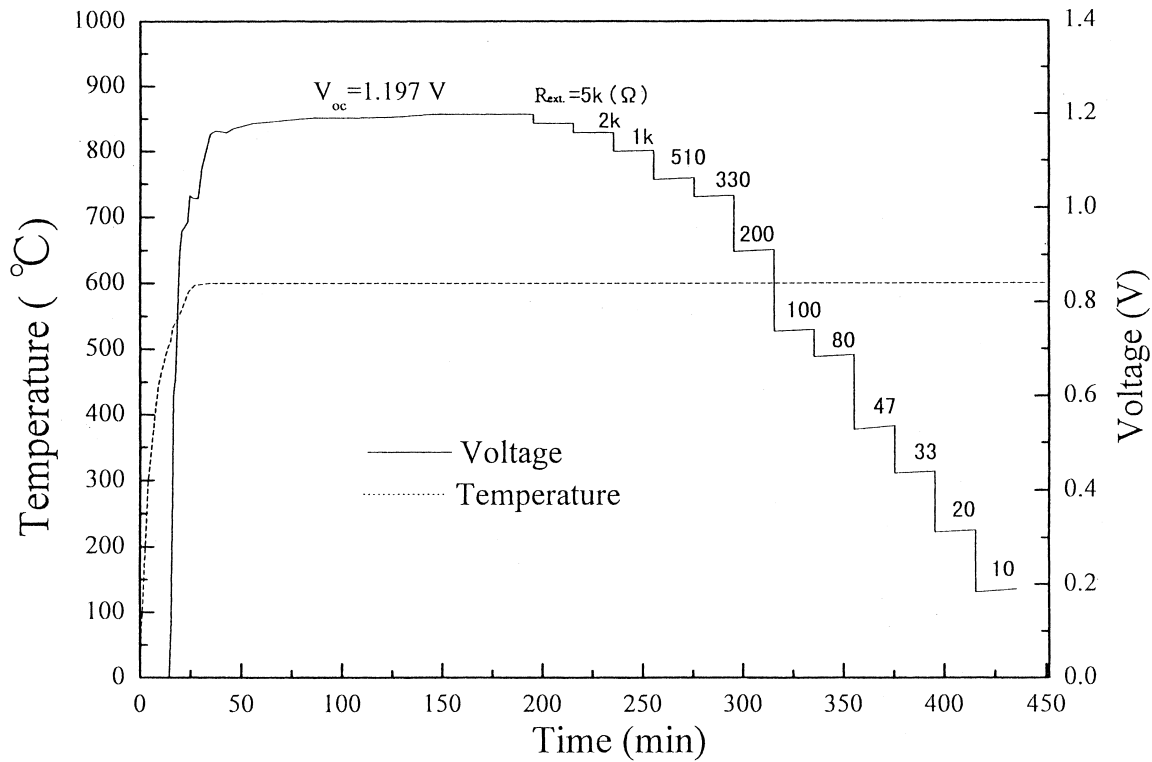


Fig. 3. Discharge under different loads for the fuel cell at 600°C using $\text{BaCe}_{0.9}\text{Y}_{0.1}\text{O}_{2.95}$ electrolyte with 1.2 mm thickness.

where E_0 is the cell EMF, and R_{int} stands for the internal resistance of the cell (electrode and electrolyte). There are two extreme cases:

$$R_{\text{ext}} = (\text{open circuit}) I_{\text{oc}} = 0, V_{\text{oc}} = E_0; \quad (\text{a})$$

$$R_{\text{ext}} = 0 (\text{short circuit}), V_{\text{sc}} = 0, I_{\text{sc}} = E_0/R_{\text{int}}, \quad (\text{b})$$

which results in following relation:

$$R_{\text{int}} = V_{\text{oc}}/I_{\text{sc}} \quad (\text{3})$$

where the subscripts oc and sc refer to open circuit and short circuit, respectively.

The current–voltage characteristics varies considerably depending on the kinds of proton conducting oxides as well as the anode materials. Fig. 4 shows the I – V characteristics of fuel cells using various electrolytes tested with nickel paste as the anode materials. The voltage loss increasing with the output current decreases in the order of $\text{SrZr}_{0.9}\text{Yb}_{0.1}\text{O}_{2.95}$ – $\text{SrCe}_{0.05}\text{Yb}_{0.05}\text{O}_{2.975}$ – $\text{BaCe}_{0.9}\text{Y}_{0.1}\text{O}_{2.95}$ in correspondence with the conductivity data by Iwahara [7]. This result suggests that, for identical electrode configurations, the voltage loss is caused by the ohmic resistance of the electrolyte.

As for the anode materials, high electronic conductivity, good catalytic function for hydrogen as well as good gas permeability are required. Some noble metals, e.g. Pt and Pd, generally qualify, but they are not suitable for practical use due to their high cost. In the present study, graphite and nickel pastes have been tested as anodes. Fig. 5 shows

the I – V characteristics of $\text{BaCe}_{0.9}\text{Y}_{0.1}\text{O}_{2.95}$ -based fuel cells using graphite and nickel anodes. The I – V characteristic of the nickel anode cell is much superior to that of the graphite anode cell. The satisfactory results for the nickel anode cells may be attributed to their efficient catalytic function and high conductivity.

A steady and stable current could be drawn from the $\text{BaCe}_{0.9}\text{Y}_{0.1}\text{O}_{2.95}$ -based fuel cell using a nickel anode. During discharge at constant current density, the terminal voltage was stable and no deterioration was observed even

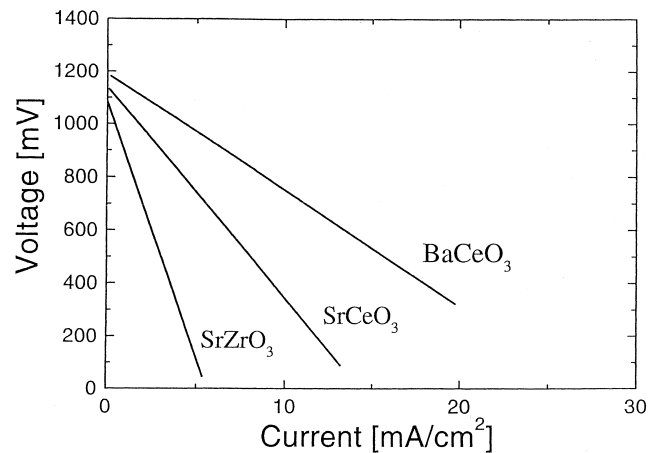


Fig. 4. I – V characteristics of the fuel cells consisting of $\text{SrCe}_{0.95}\text{Yb}_{0.05}\text{O}_{2.975}$, $\text{SrZr}_{0.9}\text{Yb}_{0.1}\text{O}_{2.95}$ and $\text{BaCe}_{0.9}\text{Y}_{0.1}\text{O}_{2.95}$ electrolytes at 600°C. Nickel anode is used.

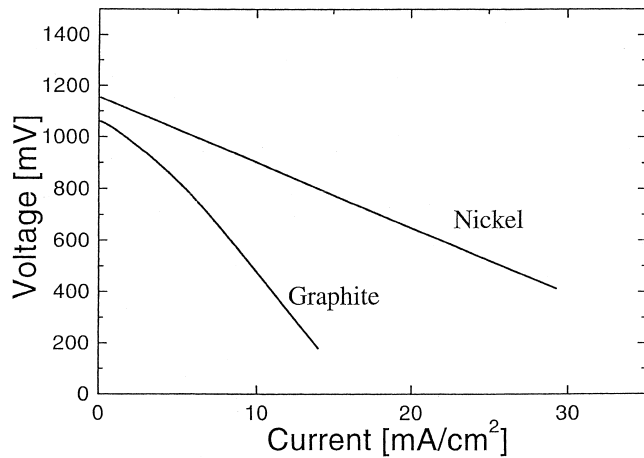


Fig. 5. I - V characteristics of the fuel cells consisting of nickel and graphite anodes at 600°C. $\text{BaCe}_{0.9}\text{Y}_{0.1}\text{O}_{2.95}$ electrolyte with 2.0 mm thickness is used.

after 10 h of continuous discharge. Fig. 6 shows the I - V characteristics of the $\text{BaCe}_{0.9}\text{Y}_{0.1}\text{O}_{2.95}$ -based cell at 600°C of the different electrolyte thickness. Current densities increased inversely with the electrolyte thickness, confirming that significant voltage losses were incurred in the solid electrolyte.

Fig. 7 shows the I - V characteristics of the $\text{BaCe}_{0.9}\text{Y}_{0.1}\text{O}_{2.95}$ -based cell of 1.2 mm electrolyte thickness at different temperatures. Current densities increase appreciably with increasing the cell temperature. This result suggests that the cell resistance associated with the electrode reaction at the negative electrode: $\text{H}_2 - 2\text{H}^+ + 2\text{e}^-$ contributes to the I - V characteristics. It is widely recognized that the performance of the hydrogen-oxygen fuel cell is improved by increasing the fuel gas pressure.

The current densities at 700 mV are used as a measure of

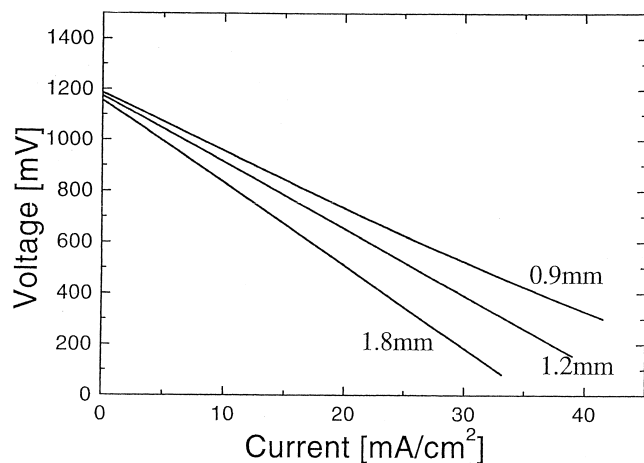


Fig. 6. I - V characteristics of $\text{BaCe}_{0.9}\text{Y}_{0.1}\text{O}_{2.95}$ -based fuel cells with a different electrolyte thickness at 600°C. Nickel anode is used.

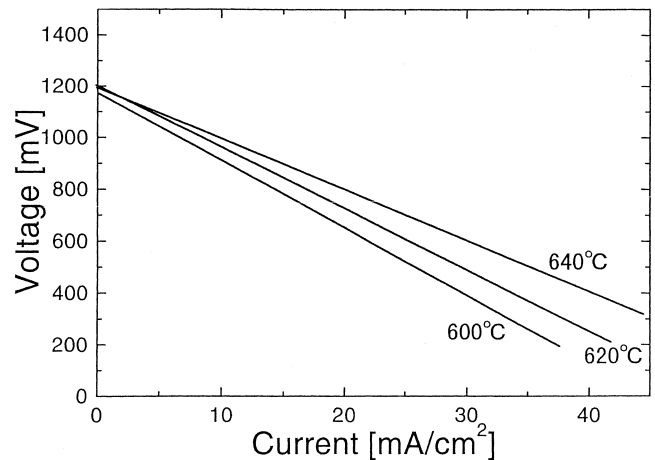


Fig. 7. I - V characteristics of $\text{BaCe}_{0.9}\text{Y}_{0.1}\text{O}_{2.95}$ -based fuel cell at 600, 620 and 640°C. Electrolyte of 1.2 mm thickness and nickel anode are used.

the performance of the fuel cells, and these are listed in Table 1 together with R_{int} values obtained from Eq. (3). The highest current density at 700 mV and the lowest R_{int} are delivered by a cell of 0.9 mm electrolyte thickness at 640°C. If the output I - V behavior obeys Ohm's law, the relative contributions of electrode reaction and proton conductivity to the R_{int} values can be evaluated by assuming that the contribution of electrolyte resistance is proportional to the electrolyte thickness, while the contribution of the electrode resistance is independent of the electrolyte thickness. From the dependence of the R_{int} values on the electrolyte thickness shown in Table 1, the contribution of the electrolyte to the R_{int} is estimated to be $130 + 30$ and $125 + 25 \Omega \text{ cm}$, at 600 and 640°C, respectively. On the other hand, the contribution of the electrode to the R_{int} are evaluated to be $10.2 + 0.8$ and $9.8 + 0.4 \Omega$ at 600 and 640°C, respectively. These results indicate that contribution of the electrolyte resistance to R_{int} is dominant to some extent over the electrode reaction. In order to develop a fuel cell which could deliver the current densities adequate for practical use, it would be required to fabricate thinner electrolyte wafers with larger proton conductivity and to further improve the anode performance.

Table 1
Current densities and internal cell resistances of the $\text{BaCe}_{0.9}\text{Y}_{0.1}\text{O}_{2.95}$ -based fuel cell with Ni anode and Ag cathode

Electrode thickness (mm)	Current density (mA cm^{-2})		Cell resistance (Ω)	
	600°C	640°C	600°C	640°C
1.8	14.3	20.8	32.9	26.0
1.2	18.2	29.2	26.6	19.6
0.9	21.0	31.6	21.7	15.2

The current densities were measured at 700 mV.

4. Summary

A hydrogen–air fuel cell consisting of proton conducting oxides as an electrolyte and hydrogen storage metals as a hydrogen source operated stably giving open circuit voltages of about 1.2 V, when the cell was maintained near a specific temperature at which hydrogen gas of about 0.1 MPa was released from the hydrogen storage metals. From the I – V characteristics for the $\text{BaCe}_{0.9}\text{Y}_{0.1}\text{O}_{2.95}$ -based fuel cells, each contribution of the electrolyte and the electrode to the internal cell resistance, R_{int} , are evaluated from the dependence of the voltage loss on the electrolyte thickness. The contribution of the electrolyte resistance to R_{int} is dominant to some extent over the electrode reaction. In order to develop the fuel cell which could deliver the current densities adequate for practical use, it would be required to fabricate thinner electrolyte wafers with larger proton conductivity and to further improve the anode performance.

Acknowledgements

This work has been supported in part by a Grant-in-Aid for Scientific Research on Priority Area (No. 299) from the Ministry of Education, Science, Sports and Culture.

References

- [1] T. Takahashi, H. Iwahara, *Energy Conv.* 11 (1971) 105.
- [2] K.W. Browell, O. Muller, *Mater. Res. Bull.* 11 (1973) 1475.
- [3] H. Iwahara, T. Esaka, H. Uchida, N. Maeda, *Solid State Ionics* 3/4 (1981) 359.
- [4] H. Iwahara, H. Uchida, S. Tanaka, *Solid State Ionics* 9/10 (1983) 1021.
- [5] N. Bonanos, B. Ellis, M.N. Mahmood, *Solid State Ionics* 44 (1991) 305.
- [6] S. Horiike, A. Kunimatsu, K. Takahiro, S. Nagata, S. Yamaguchi, *J. Alloys Comp.* 295–295 (1999) 838.
- [7] H. Iwahara, *Solid State Ionics* 28–30 (1988) 573.